Journal of Coastal Research	18	1	1–13	West Palm Beach, Florida	Winter 2002

Basis and Methods of NASA Airborne Topographic Mapper Lidar Surveys for Coastal Studies

John C. Brock†, C. Wayne Wright‡, Asbury H. Sallenger§, William B. Krabill*, and Robert N. Swift††

†USGS Center for Coastal and Regional Marine Studies
600 4th Street South
St. Petersburg, FL, 33701, USA
jbrock@usgs.gov,

‡NASA Goddard Space Flight Center
Wallops Flight Facility
Wallops Island, VA 23337, USA
wright@osb.wff.nasa.gov

§USGS Center for Coastal and Regional Marine Studies
600 4th Street South
St. Petersburg, FL 33701, USA
asallenger@usgs.gov

*NASA Goddard Space Flight Center
Wallops Flight Facility
Wallops Island, VA 23337, USA
krabill@osb1.wff.nasa.gov

††EG&G, NASA Goddard Space Flight Center
Wallops Flight Facility
Wallops Island, VA 23337, USA
swift@ao15.wff.nasa.gov

ABSTRACT

BROCK, J.C.; WRIGHT, C.W.; SALLENGER, A.H.; KRABILL, W.B., and SWIFT, R.N., 2002. Basis and methods of NASA airborne topographic mapper lidar surveys for coastal studies. *Journal of Coastal Research,* 18(1), 1–13. West Palm Beach (Florida), ISSN 0749-0208.

This paper provides an overview of the basic principles of airborne laser altimetry for surveys of coastal topography, and describes the methods used in the acquisition and processing of NASA Airborne Topographic Mapper (ATM) surveys that cover much of the conterminous US coastline. This form of remote sensing, also known as "topographic lidar", has undergone extremely rapid development during the last two decades, and has the potential to contribute within a wide range of coastal scientific investigations. Various airborne laser surveying (ALS) applications that are relevant to coastal studies are being pursued by researchers in a range of Earth science disciplines. Examples include the mapping of "bald earth" land surfaces below even moderately dense vegetation in studies of geologic framework and hydrology, and determination of the vegetation canopy structure, a key variable in mapping wildlife habitats. ALS has also proven to be an excellent method for the regional mapping of geomorphic change along barrier island beaches and other sandy coasts due to storms or long-term sedimentary processes. Coastal scientists are adopting ALS as a basic method in the study of an array of additional coastal topics. ALS can provide useful information in the analysis of shoreline change, the prediction and assessment of landslides along seacliffs and headlands, examination of subsidence causing coastal land loss, and in predicting storm surge and tsunami inundation.

ADDITIONAL INDEX WORDS: *Shoreline change, airborne laser altimetry, LaserMap.*

INTRODUCTION

During the last decade, several complementary airborne remote sensing methods have matured, resulting in significant new capabilities that are enabling advances in coastal research. Topographic information, essential for regional and local geomorphologic studies, and useful in investigations of sedimentary processes, hydrology, pedogenesis, and wildlife habitats, can now be rapidly and accurately acquired at various spatial scales by airborne laser surveying (ALS) (ACKERMANN, 1999; BUFTON, 1989). Airborne laser surveying, or "topographic lidar", is a type of remote sensing generally known as "Light Detection and Ranging" (lidar) that has undergone very rapid development during the last two decades (GARVIN, 1993; FLOOD and GUTELIUS, 1997). Airborne laser surveying herein refers to airborne topographic lidar, exclusive of other lidar methods. Numerous recent studies have demonstrated that current ALS systems have the potential to contribute within a wide range of coastal scientific investigations (CARTER and SHRESTHA, 1997; FLOOD *et al.,* 1997; GUTIERREZ *et al.,* 1998; HUISING and VAESSEN, 1997; KRABILL and SWIFT, 1982; KRABILL *et al.,* 2000; SALLENGER *et al.,* 1999a; SHRESTHA and CARTER, 1998).

00027 received 5 June 2000; accepted in revision 8 June 2001.

The advent of laser scanning as a new method for the direct, high density measurement of decimeter accuracy elevation from aircraft has been enabled by the parallel development of several incorporated techniques. Kinematic differential Global Positioning System (GPS) methods now enable the positioning of light aircraft to within several centimeters (KRABILL and MARTIN, 1987). Inertial Navigation Systems (INS) or Inertial Measuring Units (IMU) can now provide three-dimensional aircraft orientation at 64-Hz within 0.1 degree, rendering aerotriangulation based on ground data points obsolete (DELOACH, 1998). Modern lightweight laser pulse transmitters can be operated at extremely high repetition rates ranging to greater than 20,000 pulses per second, and can provide ranges from a nominal 1000 m altitude with an accuracy of 1 cm or better (BUFTON, 1989).

Combined within contemporary airborne laser mapping systems, these newly emerged technologies now enable low cost geomorphic surveys at decimeter vertical accuracy and at spatial densities greater than 1 elevation measurement per square meter. Multiple-reflection ALS is uniquely well suited to the mapping of land surfaces below even moderately dense vegetation. This technique enables the creation of "bald earth" digital elevation models in forested areas for application in investigations of geologic structure and hydrology

(KRABILL *et al.*, 1984; KRAUS and PFEIFER, 1998; LOHR, 1997; RITCHIE, 1995). In addition to sub-canopy topography, topographic lidars that capture the entire time-amplitude history of the return pulse can acquire the height and vertical structure of vegetation (BLAIR *et al.*, 1999). Unlike microwave or passive optical sensors, topographic lidars that capture the full reflected pulse can provide volumetric representations of canopy structure (BLAIR *et al.*, 1994; HARDING *et al.*, 1994; LEFSKY *et al.*, 1999).

As much recent work has demonstrated, ALS is an excellent means of mapping change along barrier island beaches and other sandy coasts (CARTER and SHRESTHA, 1997; FLOOD *et al.*, 1997; GUTIERREZ *et al.*, 1998; HUISING and VAESSEN, 1997; KRABILL and SWIFT, 1982; KRABILL *et al.*, 2000; SALLENGER *et al.*, 1999a; SALLENGER *et al.*, 1999b; SALLENGER *et al.*, 1999c; SHRESTHA and CARTER, 1998). The ability of ALS to rapidly survey long, narrow strips of terrain is very valuable in this application, as beaches are very elongate, highly dynamic sedimentary environments that undergo seasonal and long-term erosion or accretion, and are also impacted by severe storms (SALLENGER *et al.*, 1999b). Closely related applications are airborne laser mapping of flood-prone coastal fluvial zones, and the use of laser bathymeters to survey benthic change driven by hurricanes (PEREIRA and WICHERSON, 1999). Wave effects on nearshore circulation, sediment transport, and littoral zone topography may be investigated through ALS observations of sea state and surface wave displacement over continental shelves (HWANG *et al.*, 1998; TSAI and GARDNER, 1982).

OBJECTIVES

The goal of this paper is to provide an overview of the methods applied within the NASA/USGS/NOAA U.S. "lower 48" coastal mapping project (SALLENGER *et al.*, 1999b) for airborne laser surveys of coastal geomorphology. The specific objectives of this paper are:

(1) to provide the basic principles that govern the acquisition of laser ranging observations for surveys of coastal topography, and
(2) to describe the topographic lidar surveying and processing methods in use by a NASA/USGS/NOAA project that has mapped most of the conterminous US coastline.

Basis of Lidar Remote Sensing

The acronym "laser" stands for "*l*ight *a*mplification by *s*timulated *e*mission of *r*adiation" and refers to devices that rely on stimulated emission to generate narrow spectral band radiation, in contrast to conventional broad spectral band spontaneous emission of radiation governed by Planck's Law. The invention of laser transmitters capable of compressing laser energy into very short, high power density single pulses enabled range-resolved measurements (MCCLUNG and HELLWARTH, 1962), analogous to microwave *radar* ranging. By timing the two-way travel time of a laser pulse reflected off a remote target, the range to the reflector can be directly determined through division by the speed of light. The acronym "lidar" (light detection and ranging), generally refers to any remote sensing system that emits laser light and detects, ranges, or identifies remote objects based on the time-resolved sensing of light reflected or emitted through subsequent fluorescence from that object (MEASURES, 1984). By definition, lidar is a type of active remote sensing, because it incorporates an energy source to illuminate objects. Therefore, lidar differs fundamentally from passive remote sensing methods, such as multi-spectral scanning or aerial photography that rely upon reflected sunlight.

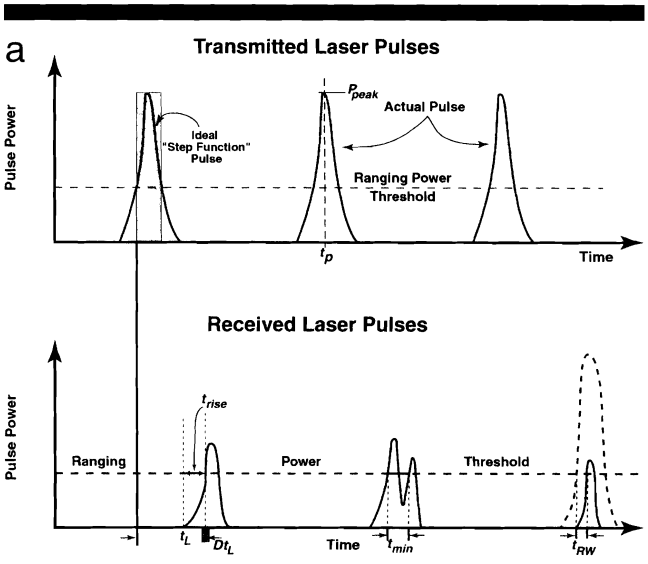

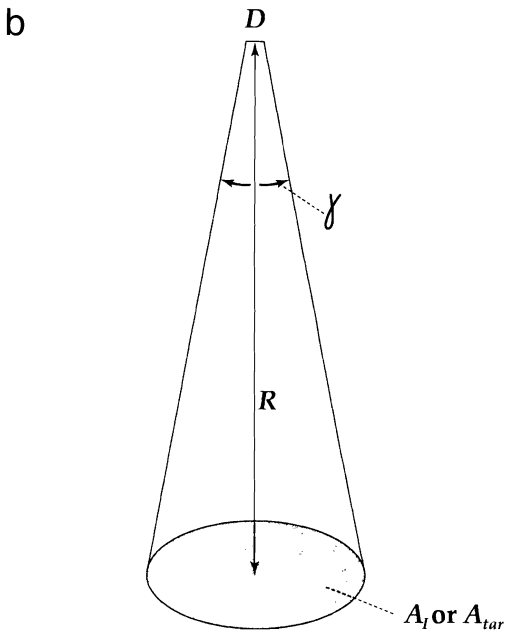

Figure 1a. Relationships between transmitted and received laser pulses (adapted from Wehr and Lohr, 1999).

Figure 1b. Geometry of a single laser shot.

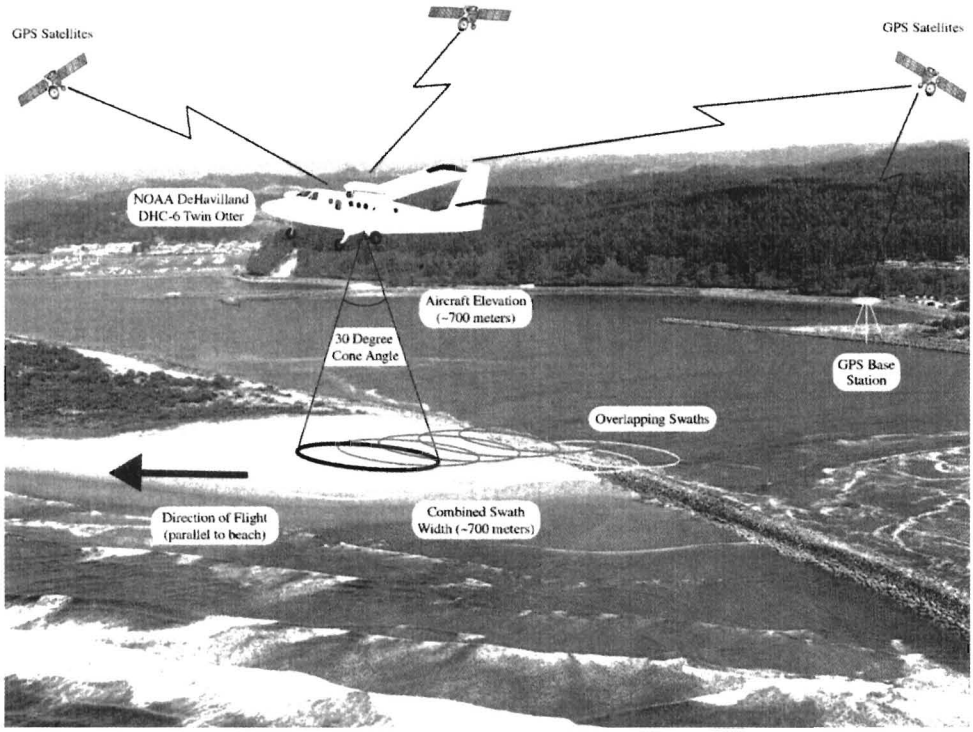

Figure 2. Aircraft laser survey in operation.

Governing Equations for Laser Ranging

Typically, *pulsed* lasers are used for ranging, because they provide tightly focused light at ultraviolet to near infrared wavelengths that is packaged into powerful radiation bursts of short duration. These characteristics are ideal for very precise distance ranging, and led to the development of scanning laser "radars" with the ability to provide range or elevation images. Airborne topographic lidar is an implementation of laser ranging that incorporates additional processing to convert the acquired ranges to an elevation field, and may be accomplished by the use of either *pulsed* or *continuous wave* lasers. In a continuous wave laser, the phase difference between the transmitted signal and the received signal backscattered from an object is used to measure ranges. In contrast, pulsed laser systems measure range by timing the two-way time-of-flight of each discrete laser light pulse. Continuous wave laser ranging for ALS will not be further discussed in this paper, because it is relatively rare in comparison to pulsed laser ranging in ALS (BALTSAVIAS, 1999; WEHR and LOHR, 1999).

A set of basic equations describe laser ranging, and apply directly to laser altimetry, under the simplifying assumption that the aircraft is perfectly horizontal, in other words, that the aircraft roll and pitch angles are zero (BALTSAVIAS, 1999; WEHR and LOHR, 1999). Definitions and units for all of the terms used in the equations described below are provided by Appendix A. The travel time t_L for an individual laser light pulse is (Figure 1a):

$$t_L = 2 \cdot \frac{R}{c} \tag{1}$$

where R is the distance between the laser transmitter and the object surface, and c is the speed of light in the medium. Given that neither the transmitted or received pulses are perfect step functions, the travel time is measured relative to a specific point on the pulse, typically a threshold amplitude on the pulse leading edge. From Equation (1), the range R to the target is:

$$R = \frac{1}{2} \cdot c \cdot t_L \tag{2}$$

The time resolution Δt_L directly controls the range resolution ΔR, which is given by:

$$\Delta R = \frac{1}{2} \cdot c \cdot \Delta t_L \tag{3}$$

The minimum detectable separation between reflecting targets along the pulse path, or the multiple target range resolution R_{min},

$$R_{min} = c \cdot \frac{t_{min}}{2} \tag{4}$$

is similarly a function of the minimum time difference t_{min} between two received echoes. In general, very short duration, high amplitude laser pulses with a short pulse rise-time enhance multiple target discrimination in the reflected laser waveform.

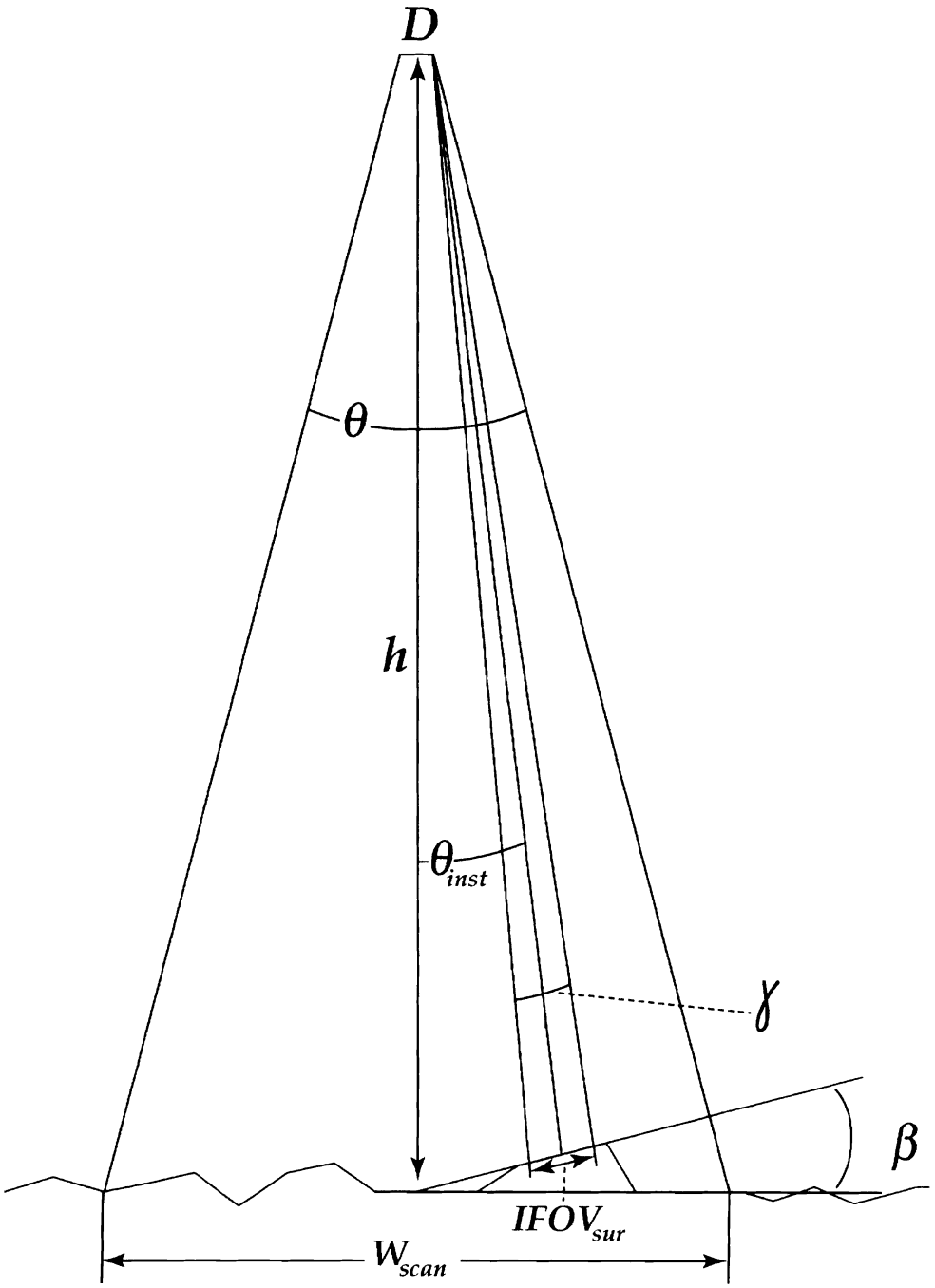

Figure 3. Diagram of the geometry of a laser swath.

The maximum range is determined by the longest time interval that can be recorded by the laser system timer, and also by laser energy attenuation during propagation. The absolute ranging accuracy σ_R depends on the pulse rise time t_{rise} and the overall system signal-to-noise ratio S/N (WEHR and LOHR, 1999):

$$\sigma_R \sim \frac{c}{2} \cdot t_{rise} \cdot \frac{1}{\sqrt{\frac{S}{N}}} \tag{5}$$

The peak laser pulse power P_{peak} increases for a given laser energy E as the pulse duration t_p decreases:

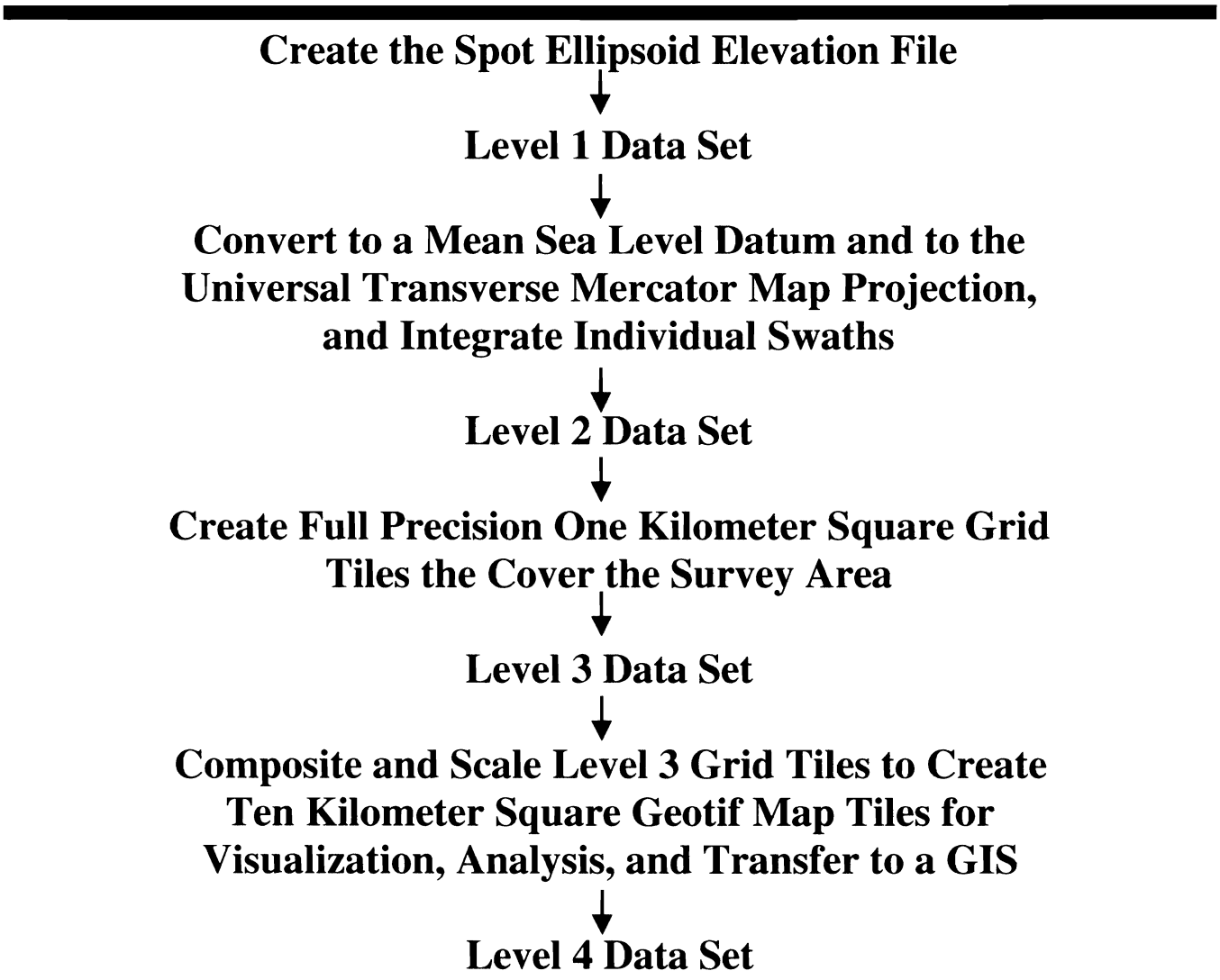

Figure 4. Processing flow for airborne laser mapping data.

$$P_{peak} = \frac{E}{t_p} \tag{6}$$

and the average pulse power P_{av} is the product of the laser energy and the pulse repetition rate F:

$$P_{av} = E \cdot F \tag{7}$$

Similarly, if the pulse duration is held constant, the peak laser pulse power will decrease as the pulse repetition rate increases:

$$P_{peak} = \frac{P_{av}}{t_p \cdot F} \tag{8}$$

Assuming a circular target that is a perfectly diffuse reflector (Figure 1b), the illuminated area A_I is calculated as:

$$A_I = \frac{\pi}{4} \cdot (D + R \cdot \gamma)^2 \tag{9}$$

where D is the laser aperture width, R is the range, and γ is the laser beam divergence. The power density ϕ_{tar} within the illuminated area A_I is a function of the transmitted power P_T, and the atmospheric transmission M:

$$\Phi_{tar} = \frac{P_T}{A_I} \cdot M \tag{10}$$

The total power reflected from the target P_{refl} is:

$$P_{refl} = \frac{\rho}{\pi} \cdot \Phi_{tar} \cdot A_{tar} \tag{11}$$

where ρ is the target reflectance, and the target area A_{tar}, a function of the target diameter D_{tar}, is given by:

$$A_{tar} = \frac{\pi \cdot D_{tar}^2}{4} \tag{12}$$

The relationship between transmitted and received power, known generally as the range equations, is completed by calculating the resulting reflected pulse power received at the

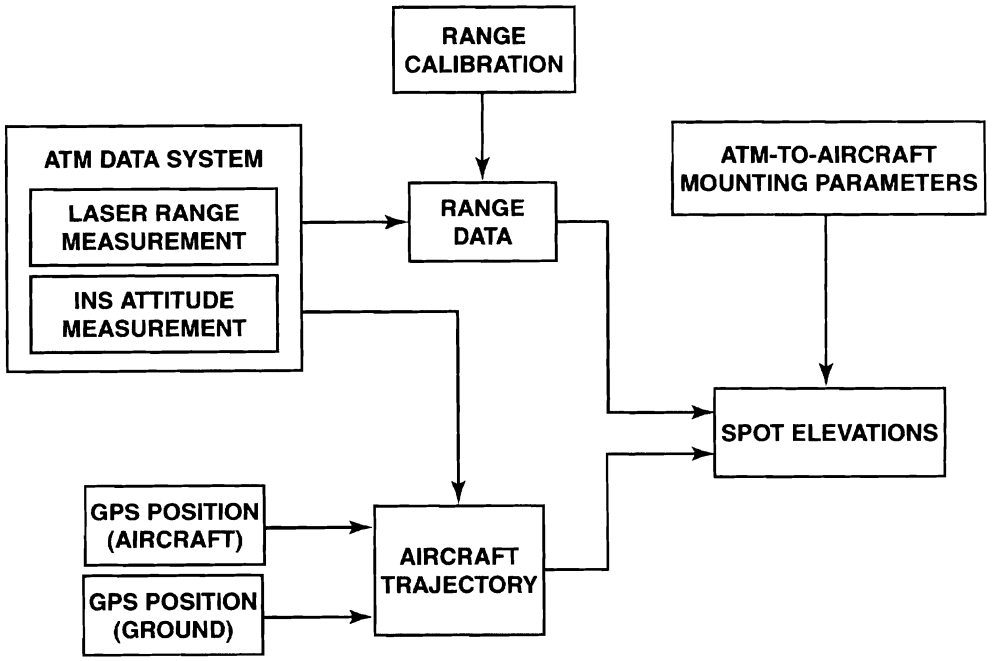

Figure 5. Level 1 data creation diagram.

collector, P_{rec} with a optical receiving area A_{rec}, and an aperture diameter D_{rec}:

$$P_{rec} = P_{refl} \cdot M \cdot \frac{A_{rec}}{R^2} \tag{13}$$

and

$$A_{rec} = \frac{\pi \cdot D_{rec}^2}{4} \tag{14}$$

Combining Equations 9 through 14 above, and assuming that the illuminated area A_l is equal to the target area A_{tar}, and that D_{rec} is minute and negligible in comparison to $R \cdot \gamma$, Equation 13 reduces to (BALTSAVIAS, 1999):

$$P_{rec} = \rho \frac{M^2 \cdot A_{rec}}{\pi \cdot R^2} \cdot P_T \tag{15}$$

The NASA ATM Laser Mapping System

Although laser surveying for terrain and vegetation elevation measurements can be carried out from satellite, airborne, or fixed platforms, only the NASA Airborne Topographic Mapper (ATM) aircraft-mounted system is discussed in this paper. The mapping configuration used by NASA for Airborne Topographic Mapper surveys of coastal terrain includes a twin engine light aircraft equipped with a lidar instrument, INS, and GPS, which is operated in tandem with a GPS basestation, usually sited at the airport used to stage the flights (Figure 2). In coastal applications, the aircraft flies along the coast at a height of about 700 meters, surveying a ground swath directly below the aircraft. The aircraft position throughout the survey flight is recorded by an onboard geodetic grade GPS receiver. The aircraft GPS signals are later combined with signals concurrently collected by a nearby GPS base station for differential kinematic GPS post-processing to determine the aircraft flight trajectory to within 5 centimeters.

Airborne laser mapping may be carried out at night, but for flight safety, NASA ATM coastal ALS operations are normally confined to daylight hours, and timed to coincide with low tide to maximize coverage of the beach face. Use of lasers with sufficient pulse power to overcome attenuation in a clear atmosphere at flying altitudes less than 1000 meters minimizes the importance of atmospheric effects on laser signal intensity. However, where present, fog and heavy precipitation can cause inaccurate elevation measurement due to the early reflection of pulses within the atmosphere. A range of aircraft are suitable for ALS, given installation of a port in the base of the fuselage and power supply modification to match the lidar instrument. The twin engine aircraft used by the NASA/USGS/NOAA cooperative beachmapping project was selected based on maneuverability, high payload capacity, long range, and the ability to cruise at airspeeds near 100 knots.

Airborne topographic lidars use a variety of possible scanning mechanisms to provide a swath of measurements beneath the airborne platform, rather than a single profile line, as all scanners act to deflect laser pulses across the aircraft ground track. For example, an oscillating mirror placed in the path of the laser emission creates a zigzagging bi-directional raster pattern. In contrast, rotating polygon and multi-faceted mirrors give unidirectional scans of parallel lines, optical fibre designs can produce a "pushbroom" scan of lines parallel

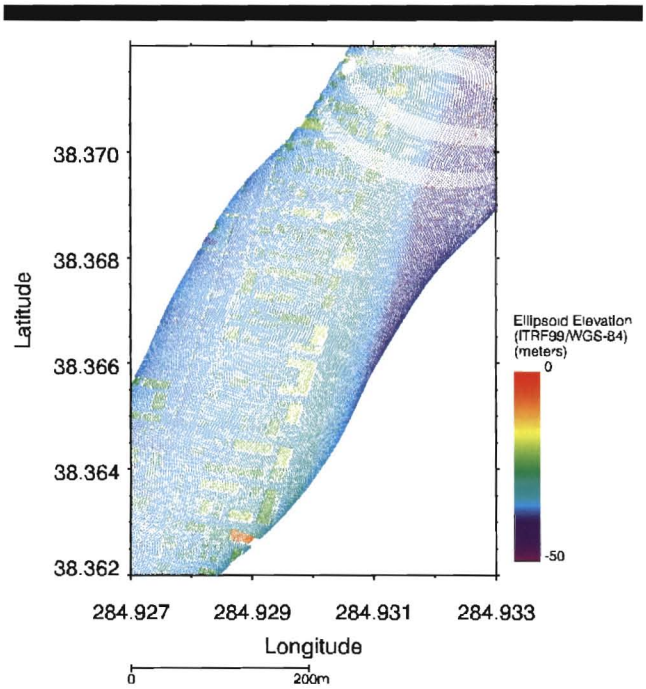

Figure 6a. Plot of point elevations referenced to ITRF99/WGS-84 from a Level 1 NASA ATM lidar file.

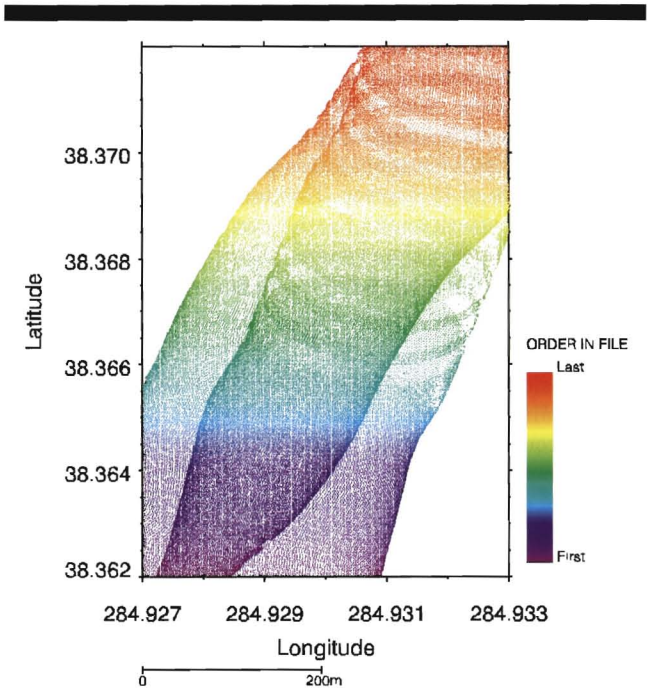

Figure 7a. Plot of the points in a Level 2 file, color-coded based on position in the file from first (blue) to last (red).

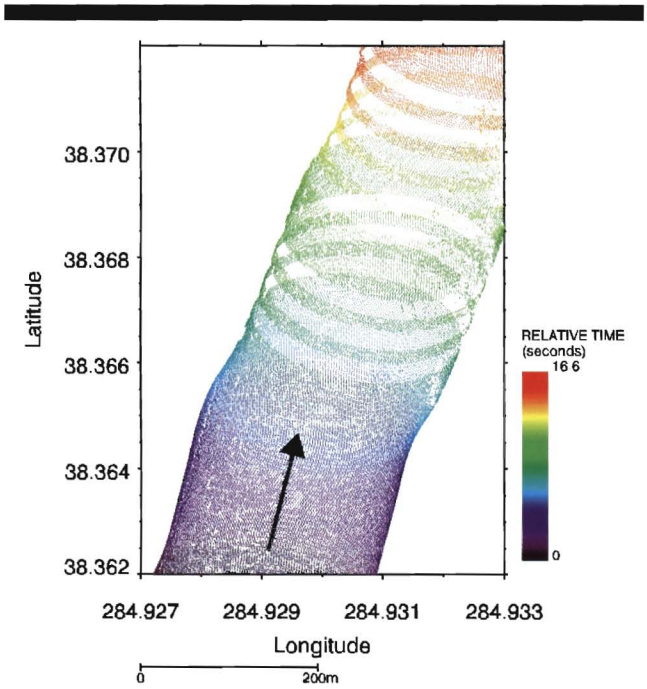

Figure 6b. Plot of the points in a Level 1 NASA ATM lidar file, color-coded based on the position in the file from first (blue) to last (red).

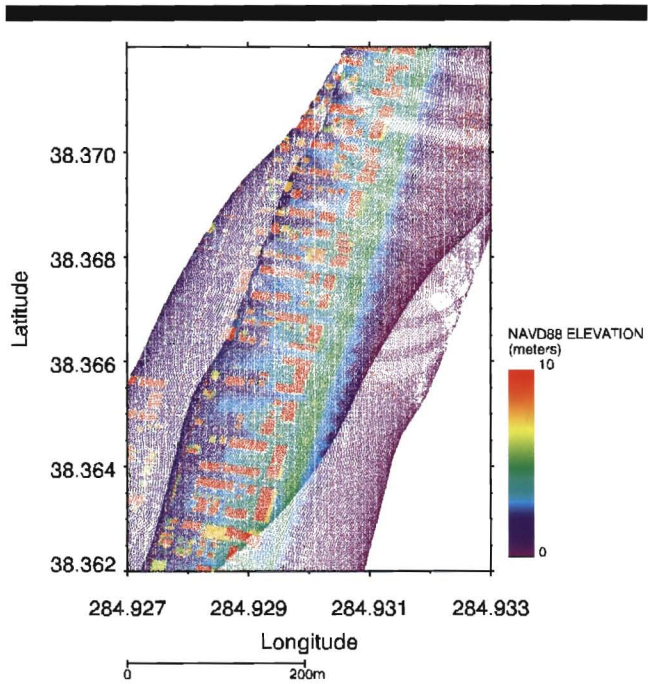

Figure 7b. Plot of point elevations referenced to NAD-83/NAVD88 from a Level 2 file.

to the flying direction, and nutating mirrors produce an elliptical scan pattern also known as a "Palmer" scan. The topographic lidar data collected over US coasts (SALLENGER *et al.*, 1999b) by the NASA/USGS/NOAA project has been acquired by use of the elliptically scanning NASA ATM, whose scan mirror has a rotational axis angle of 45 degrees and a off-nadir angle of 15 degrees. This instrument creates an elliptical scan pattern on the Earth's surface with a swath that is roughly one half of the nominal 700 meter aircraft altitude, approximately 350 meters wide (KRABILL *et al.*, 2000).

Governing Equations for Airborne Laser Scanning

The basic formulas and relations that govern laser ranging apply to airborne laser altimetry. However, the addition of a scanner coupled to the laser transmitter and uncertainties in three-dimensional aircraft positioning introduce the need for additional equations to describe the ranging observations acquired by airborne laser scanning. Relations between ALS variables, such as the laser footprint, swath width, and the shots per scan line are provided next. Together with equations that provide overall survey characteristics, such as the shot spatial density, the total area surveyed, and total data volume, these relations are useful both in planning ALS missions and in comparing the performance of different ALS systems (BALTSAVIUS, 1999; WEHR and LOHR, 1999).

The minimum laser beam divergence, which gives the narrowest possible laser footprint, also called the diffraction-limited instantaneous field of view ($IFOV_{diff}$), is a function of the laser wavelength λ and the laser aperture width D (Figure 3):

$$IFOV_{diff} = 2.44 \cdot \frac{\lambda}{D} \tag{16}$$

The instantaneous field of view during a laser survey, $IFOV_{sur}$, or the laser footprint size, increases from this minimum value with increasing aircraft altitude, and over perfectly flat terrain (Figure 3) it may be calculated as:

$$IFOV_{sur} = 2 \cdot h \cdot \tan\left(\frac{\gamma}{2}\right) \tag{17}$$

where h is the slant range flying height above the terrain, and γ is the laser beam divergence. Admitting the additional complications of inclined terrain and variable instantaneous scan angle, the equation for $IFOV_{sur}$ becomes (Figure 3):

$$IFOV_{sur} = \left\{\left[\cos(\theta_{inst} + \beta) + \sin(\theta_{inst} + \beta) \cdot \tan\left((\theta_{inst} + \beta) + \frac{\gamma}{2}\right)\right] \times 2 \cdot h \cdot \sin\left(\frac{\gamma}{2}\right)\right\} \Big/ \left[\cos\left(\theta_{inst} + \frac{\gamma}{2}\right)\right] \tag{18}$$

where θ_{inst} is the instantaneous scan angle, and β is the inclination angle of the local planar terrain surface. The width of the scanned swath beneath the aircraft W_{scan} is defined by the aircraft altitude above the terrain h, and the laser scan angle or field of view θ:

$$W_{scan} = 2 \cdot h \cdot \tan\left(\frac{\theta}{2}\right) \tag{19}$$

Given the time during which data was acquired for each strip during a survey T_{sur} and the percentage of overlap between strips q, in addition to the scan width W_{scan} and the flying speed υ, the total area covered by an airborne laser survey A_{sur} is:

$$A_{sur} = W_{scan} \cdot \upsilon \cdot T_{sur} \left[(n - 1)\left(1 - \frac{q}{100}\right) + 1\right] \tag{20}$$

The overall point density d within an entire survey is given by:

$$d = \frac{F \cdot n \cdot T_{sur}}{A_{sur}} \tag{21}$$

and the aircraft displacement in the time interval between sending and receiving a laser pulse s is calculated based on υ, the flying speed over the terrain, the range R, and the speed of light c:

$$s = \frac{2 \cdot \upsilon \cdot R}{c} \tag{22}$$

Finally, the total volume of data C acquired by an ALS survey may be calculated as the product of the pulse repetition rate F, the total data acquisition time T_f, and the number of bytes per laser shot P_{bytes} (BALTSAVIAS, 1999; WEHR and LOHR, 1999):

$$C = F \cdot T_f \cdot P_{bytes} \tag{23}$$

Processing of NASA Airborne Topographic Mapper Survey Data

Distillation of extremely dense ALS elevation data sets into a form that is readily useable in scientific analyses and Geographic Information Systems without loss of essential information is a technical challenge. Although there are many valid solutions (BROCK *et al.*, 1999; CARTER *et al.*, 1997; PETZOLD *et al.*, 1999), the approach described herein is that adopted by NASA (Level 1 processing) and the USGS Center for Coastal and Regional Marine Studies (CCRMS) (Level 2, Level 3, and Level 4 processing) for NASA ATM surveys. A software package called LaserMap is being developed at the USGS/CCRMS to enable a systematic multi-tiered approach to the preparation of information products based on the Level 1 lidar files provided by NASA. LaserMap supports the creation of point elevation data files in relevant reference systems (Level 2), enables the gridding of entire surveys into compact tiles at full vertical and horizontal accuracy (Level 3), and allows the assembly of large elevation image maps over selected regions (Level 4)(Figure 4).

Level 1 Processing

Determination of the spot elevation of a location on the earth's surface through aircraft laser altimetry requires that the laser range information be combined with the instantaneous location of the aircraft (Figure 5). Given laser range errors of several centimeters, the aircraft location at all times throughout a survey flight must be known to within about 5 centimeters in order to measure topography to the desired accuracy of 10 centimeters. This accuracy is achieved through the use of kinematic GPS techniques that rely upon comparison of the dual frequency carrier-phase-derived position data

obtained at both a fixed base station receiver, and at a mobile receiver in the aircraft (KRABILL *et al.,* 2000).

Airborne laser mapping systems require at least 2 types of calibration, a "range walk" correction (Figure 1a), and an instrument mounting bias calibration. "Range walk" refers to a systematic error that arises as variable amplitude return pulses are encountered by the leading edge discriminator used in timing the laser range measurement. During pre- and post-mission "range walk" calibrations, the outgoing laser beam is reflected horizontally towards a target at a known distance from the laser transmitter. Range measurements are acquired while the laser strength is varied to collect data that describe the relationship between laser signal amplitude and range variation. This ground calibration data is used in post-flight processing to remove the systematic error in range that results from variation in amplitude of the laser return signal (KRABILL *et al.,* 2000).

A second calibration must be applied to correct for the angular mounting bias of the ATM instrument relative to the Inertial Navigation System (INS). First, the aircraft collects data over a flat surface or well-surveyed reference site, such as a large parking lot or airport ramp. The resulting range measurements are compared to ranges determined by computations based on the determined position of the GPS antenna, the position of the scanner mirror, INS-derived pitch, roll, and heading data, and a model of the scanner measurement system. This procedure allows determination of the angular mounting bias and the required calibration (KRABILL *et al.,* 2000).

The aircraft trajectory is determined through differential kinematic GPS techniques (KRABILL and MARTIN, 1987) that involve the differencing of ranges obtained through reception of the GPS dual frequency carrier-phase signals at both a fixed base station receiver and a mobile aircraft receiver. The airborne GPS receiver maintains continuous reception by avoiding bank angles greater than 10 degrees throughout all flights, and GPS data sets are collected within 45 minutes pre- and post-flight with the aircraft on the ground and adjacent to the fixed baseline receiver. These stationary data sets, and data describing local meteorological conditions, are stored and later used in processing the inflight survey data. Subsequent to each mission, point-to-point range difference solutions for the aircraft trajectories for each flight are calculated, using precise *post facto* ephemeris data for the GPS constellation. Combination of the laser range data with the aircraft trajectories provides survey results expressed in IERS (International Earth Rotation Service) Terrestrial Reference Frame 1999 (ITRF99) coordinates, referenced to the WGS-84 ellipsoid. These results are possible because WGS-84 and ITRF99 geodetic systems are equivalent within the centimeter range worldwide, and may be regarded as equivalent for mapping and charting purposes (NIMA, 2000).

Level 2 Processing

Decimeter vertical accuracy ALS survey elevation data are available at the completion of Level 1 processing (SALLENGER *et al.,* 1999a). However, Level 1 ALS data is not readily useful to coastal scientists for several reasons. First, ITRF99/WGS-84 is not the reference frame typically used by the coastal science community (Figure 6a), nor is it referenced to a sea level datum, thus it is generally necessary to undertake a coordinate conversion. Second, the Level 1 data exists in scanned order for each separate flightline over the survey area (Figure 6b). In the case of the NASA ATM, the elliptical scan observations acquired during the rearward-looking portion of an individual scan pass across the same sites that were surveyed during the forward-looking portion of a slightly earlier scan (for example, see the northern portion of Figure 6b). Thus, on spatial scales less than several hundred meters, the observations as scanned do not have a simple ordering in terms of ground position. Essentially, Level 2 processing converts the Level 1 data into a pseudo-raster form that greatly simplifies further analysis.

Level 2 processing begins with the extraction of the ITRF99/WGS-84 elevations and spot latitude and longitude positions from each relevant Level 1 flightline's data set within the geographic region of interest. Depending on the general compass bearing of the coastline, the NASA ATM data set for each flightline is converted from its original elliptical scan geometry by ranking to an order in which consecutive point locations progress in latitude (north-south trending coasts) or longitude (east-west trending coasts) order (Figure 7a). The ITRF99/WGS-84 coordinates for the spot locations for each individual flightline are converted to the NAD-83 horizontal datum using the GRS-80 ellipsoid. Next, geoid heights are calculated by use of the National Geodetic Survey's GEOID99 model, and the ellipsoid and geoid heights are summed to yield orthometeric elevations relative to NAVD88, a vertical sea level datum (ZILKOSKI *et al.,* 1992). At this step any error that may exist in the GEOID99 model for the geographic area of interest will be introduced into the final NAVD88 lidar elevation data set (DANIELS, 2000). The merging of elevation points for each separate flightline into integrated data sets for an entire survey completes the Level 2 processing. The resulting Level 2 data sets have an east-west or north-south sorted pseudo-raster geometry, are referenced to the NAD-83 horizontal datum and the NAVD88 vertical datum, and typically collapse observations from multiple swaths captured during several flight swaths on a single day into one common data set (Figure 7b).

Level 3 Processing

The purpose of Level 3 processing is to create a gridded version of the Level 2 data set that efficiently covers the Level 2 survey area and involves no loss of the true vertical and horizontal accuracy of the elevation data contained in the Level 2 file. The first step in Level 3 processing is the determination of the full latitude and longitude ranges of the Level 2 data set under analysis. The area covered by a NASA ATM coastal topographic lidar survey is typically a narrow, elongate swath that may trend diagonally across a large region. As such, it is not practical or efficient to simply create grid files that cover the entire region described by the latitude and longitude ranges of a given Level 2 survey. The creation of one kilometer square grid tiles only over the actual survey

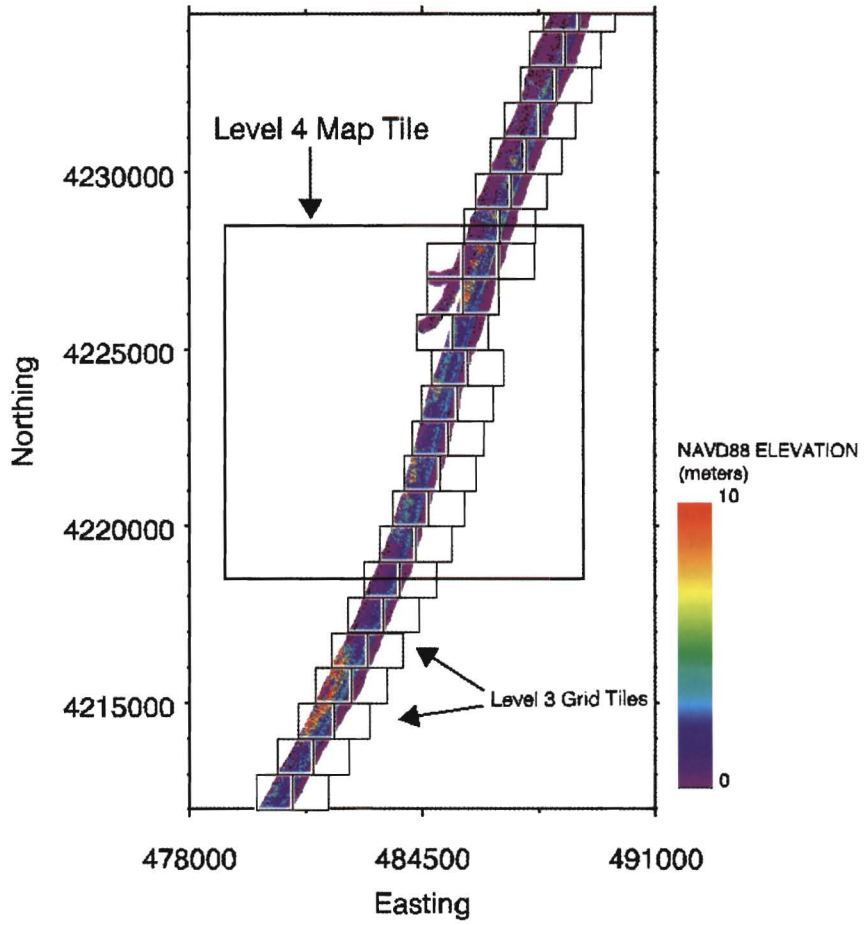

Figure 8. Plot of the Level 2 elevation values in a NASA ATM survey, overlain by squares showing the relative locations of the Level 3 grid tiles automatically generated for this data set. A Level 4 map tile positioned to cover a region of interest is also depicted.

area within Level 3 processing resolves this problem, while allowing for gridding of the entire Level 2 data set.

Starting in the Level 2 survey region's southwest corner, a series of one kilometer by one kilometer grid tiles are defined that cover just the actual survey area within the geographic region described by the survey's full latitude and longitude extent (Figure 8). Beginning with the southwestern-most grid tile, the spot elevation points for each tile are sequentially extracted from the Level 2 file. In order to minimize edge effects between grid tiles, points within a buffer just outside the grid tile margins are included in the creation of each grid tile. The set of Level 2 points for a given Level 3 grid tile are first used to create a Delaunay triangulation. This triangulation is used together with the point elevation values to create each one kilometer square grid tile at full 1 millimeter vertical precision and at a minimum 1 meter grid cell size. Each one kilometer square component grid tile is written to the Level 3 file in sequence, along with an imbedded header that provides the geographic position of each grid cell in each grid tile.

Level 3 processing results in a gridded data set at the full vertical precision of the NASA ATM Level 2 data set used to create it. Although the actual vertical accuracy of the Level 2 elevation data points is roughly 10 centimeters, the point elevation values are recorded at an internal Level 2 file precision of 1 millimeter, and this vertical precision is maintained in the Level 3 file. In the Level 2 file, the horizontal precision in positioning is roughly 10 centimeters, given that both latitude and longitude are recorded as microdegrees. However, given a maximum error in aircraft attitude of about 0.1 degree and a nominal survey altitude of 800 meters, the actual horizontal accuracy in point position is about 1.4 meters. Consequently, the 1 meter grid cell dimension used in the creation of standard LaserMap Level 3 grid tiles does not entail any real loss of accuracy in the horizontal positioning of the NASA ATM data set.

Level 4 Processing

The Level 3 file for a survey contains a series of adjacent component grid tiles that automatically follow and cover any irregular survey area. Although efficient for the storage of a gridded version of a Level 2 file, a Level 3 file is not appropriate for the direct visualization of topography. The creation of large map tiles for visual interpretation or regional quantitative analysis is the purpose of Level 4 processing.

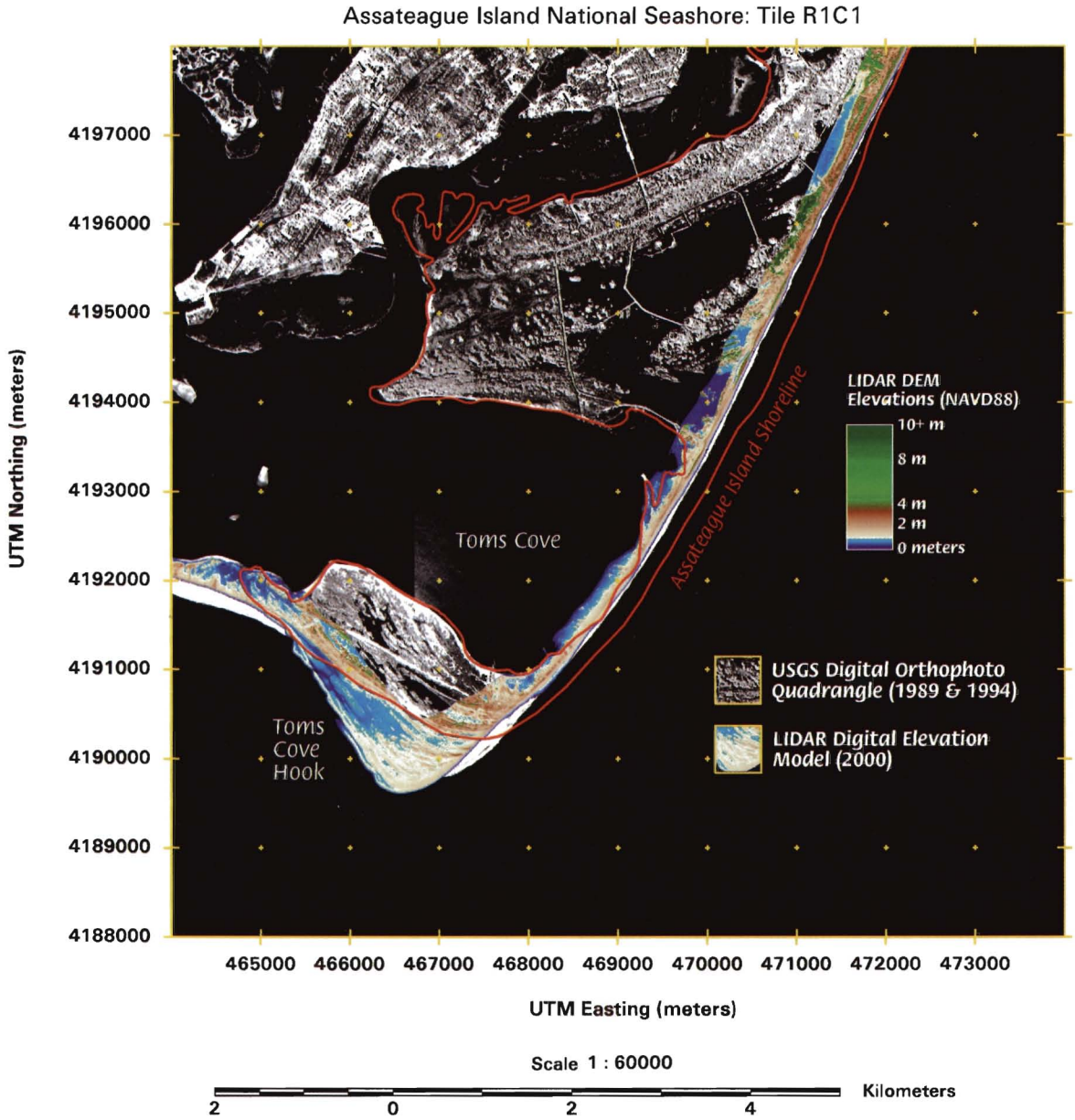

Figure 9. A Level 4 geotiff map tile containing NASA ATM topography over the southern tip of Assateague Island merged with a Digital Qrthophotograph Quadrangle and a vector shoreline in a Geographic Information System.

The composite survey region covered by the component grid tiles within a Level 3 file generally is irregular in shape. However, the geographic location of each Level 3 grid cell is captured within imbedded headers internal to the Level 3 file. This allows the Level 3 component grids to be assembled into larger map tiles that have been defined to cover a region of interest. At Level 3, the placement of the component grid tiles is determined by the coverage area of the Level 2 data itself, in order to allow efficient gridding and data storage. In contrast, at Level 4 the analyst defines regions for image map creation based on scientific objectives.

Prior to the initiation of the Level 4 processing of a Level 3 data set, an analyst defines one or more ten kilometer square map regions that cover the desired study area (Figure 8). The cornerpoints of these ten kilometer square map tiles are entered into a file that is called by the LaserMap Level 4 processing module in order to guide map tile creation based on a Level 3 file. If multiple lidar surveys have been conducted over a region, a Level 3 file may be created for each, and Level 4 processing may be carried out for each Level 3 file, using a fixed set of Level 4 map tile locations.

In creating a given map tile, the Level 4 module reads through the Level 3 file, and places either whole or partial Level 3 grid tiles into the Level 4 map tile, based on the

geographic locations of the Level 3 grid tile cells relative to the desired Level 4 map tile region. Level 4 map tiles cover 10 kilometer square areas that are much wider than the swath width of most NASA ATM coastal lidar surveys, typically less than one kilometer in width. As a result, Level 4 map tiles often contain significant regions outside the actual survey area, and to restrict file size, Level 4 map tiles are scaled to centimeter vertical precision, rather than the millimeter vertical precision of the parent Level 3 file. Note that the vertical precision of the Level 4 map tiles is still about tenfold higher than the actual vertical accuracy of the lidar elevation measurements, approximately ten centimeters.

LaserMap supports the creation of Level 4 map tiles as geotiff files, a generic image file format that includes information on image georectification, and that is readable by most Geographic Information System (GIS) software packages. Accordingly, Level 4 map tiles may be conveniently used to insert lidar topography as a GIS data layer (Figure 9), and may also be used by special purpose analysis programs. At present, methods are under development that use Level 4 map tiles in shortline definition, three-dimensional geomorphic change analysis, and in the mapping of plant communities and wildlife habitats.

SUMMARY

Based on its capacity for carefully-timed high resolution regional surveys keyed to natural processes, ALS is becoming a fundamental tool for coastal scientists within coastal studies. This paper provides a set of basic equations that describe laser ranging, and its implementation within the airborne laser scanning of topography. A description of the processing steps used by NASA and the USGS to extract scientifically useful information from the vast number of observations that are obtained through NASA ATM surveys is provided. The multi-tiered lidar processing approach outlined here supports the geometric, reference system, and file structure transformations that are required for most coastal applications of ALS. This approach is being incorporated in a software package called LaserMap that creates lidar data products that may be directly inserted into a Geographic Information System, or used within specialized analysis programs designed to extract landscape information for coastal studies.

ACKNOWLEDGMENTS

The USGS Coastal and Marine Program of the Geologic Division funded this work as a component of the National Assessment of Coastal Change Project. J. C. Brock thanks R. Morton and T. Edgar for candid and thoughtful reviews of an early draft of this paper, and gratefully acknowledges D. Hickey, A. Nayegandhi, and M. Harris for assistance in the preparation of figures.

LITERATURE CITED

ACKERMANN, F., 1999. Airborne laser scanning—present status and future expectations, *ISPRS Journal of Photogrammetry and Remote Sensing,* 54, 64–67.

BALTSAVIAS, E.P., 1999. Airborne laser scanning: existing systems and firms and other resources, *ISPRS Journal of Photogrammetry and Remote Sensing,* 54, 164–198.

BLAIR, J.B.; COYLE, D.B.; BUFTON, J.L., and HARDING, D.J., 1994. Optimization of an airborne laser altimeter for remote sensing of vegetation and tree canopies, *International Geoscience and Remote Sensing Symposium '94, Surface and Atmospheric Remote Sensing: Technologies, Data Analyses and Interpretation,* 2, 939–941.

BLAIR, J.B.; RABINE, D.L., and HOFTON, M.A., 1999. The laser vegetation imaging sensor: a medium-altitude, digitisation-only, airborne laser altimeter for mapping vegetation and topography, *ISPRS Journal of Photogrammetry and Remote Sensing,* 54, 115–122.

BROCK, J.C.; SALLENGER, A.H.; KRABILL, W.B.; SWIFT, R.N.; MANIZADE, S.S.; MEREDITH, A.; JANSEN, M., and ESLINGER, D., 1999. Aircraft laser altimetry for coastal process studies, *Proceedings of the 4th International Symposium on Coastal Engineering and Science of Coastal Sediment Processes,* 3, 2414–2428.

BUFTON, J.L., 1989. Laser altimetry measurements from aircraft and spacecraft, *Proceedings of the IEEE,* 77(3), 463–477.

CARTER, W.E. and SHRESTHA, R.L., 1997. Airborne laser swath mapping: Instant snapshots of our changing beaches, *Proceedings of the Fourth International Conference on Remote Sensing for Coastal and Marine Environments,* Orlando, 298–307.

DANIELS, R.C., 2000. Datum conversion issues with lidar spot elevation data, *Photogrammetric Engineering and Remote Sensing, in press.*

DELOACH, S., 1998. Photogrammetry: A revolution in technology, *Professional Surveyor,* March 1998, 8–14.

FLOOD, M. and GUTELIUS, W., 1997. Commercial implications of topographic terrain mapping using scanning airborne laser radar, *Photogrammetric Engineering and Remote Sensing,* 63(4), 327–366.

FLOOD, M.; GUTELIUS, W., and ORR, M., 1997. Terrain mapping, *Earth Observations Magazine,* February 1997, 40–42.

GARVIN, J.B., 1993. Mapping new and old worlds with laser altimetry, *Photonics Spectra,* April 1993, 89–94.

GUTIERREZ, R.; GIBEAUT, J.C.; CRAWFORD, M.M.; MAHONEY, M.P.; SMITH, S.; GUTELIUS, W.; CARSWELL, D., and MACPHERSON, E., 1998. Airborne laser swath mapping of Galveston Island and Bolivar Peninsula, Texas, *Proceedings of the Fifth International Conference on Remote Sensing for Marine and Coastal Environments,* San Diego, 236–243.

HARDING, D.J.; BLAIR, B.J.; GARVIN, J.B., and LAWRENCE, W.T., 1994. Laser altimetry waveform measurement of vegetation canopy structure, *International Geoscience and Remote Sensing Symposium '94, Surface and Atmospheric Remote Sensing: Technologies, Data Analyses and Interpretation,* 2, 1251–1253.

HUISING, E.J. and VAESSEN, E.M.J., 1997. Evaluating laser scanning and other techniques to obtain elevation data on the coastal zone, *Proceedings of the Fourth International Conference on Remote Sensing for Marine and Coastal Environments,* Orlando, 510–517.

HWANG, P.A.; WALSH, E.J.; KRABILL, W.B.; SWIFT, R.N.; MANIZADE, S.S.; SCOTT, J.F., and EARLE, M.D., 1998. Airborne remote sensing applications to coastal wave research, *Journal of Geophysical Research,* 103(C9), 18,791–18,800.

KRABILL, W.B.; COLLINS, J.G.; LINK, L.E.; SWIFT, R.N., and BUTLER, M.L., 1984. Airborne laser topographic mapping results, *Photogrammetric Engineering and Remote Sensing,* 50(6), 685–694.

KRABILL, W.B. and SWIFT, R.N., 1982. *Preliminary results of shoreline mapping investigations conducted at Wrightsville Beach, North Carolina, U.S. Army Corps of Engineers Survey Requirements Meeting.* Vicksburg, Mississippi, 261–280.

KRABILL, W.B. and MARTIN, C.F., 1987. Aircraft positioning using global positioning system carrier phase data, *Navigation,* 34, 1–21.

KRABILL, W.B.; WRIGHT, C.W.; SWIFT, R.N.; FREDRICK, E.B.; MANIZADE, S.S.; YUNGEL, J.K.; MARTIN, C.F.; SONNTAG, J.G.; DUFFY, M., HULSLANDER, W., and BROCK, J.C., 2000. Airborne laser mapping of Assateague National Seashore beach, *Photogrammetric Engineering and Remote Sensing,* 66(1), 65–71.

KRAUS, K. and PFEIFER, N., 1998. Determination of terrain models in wooded areas with airborne laser scanner data, *ISPRS Journal of Photogrammetry and Remote Sensing,* 53, 193–203.

LEFSKY, M.A.; COHEN, W.B.; ACKER, S.A.; PARKER, G.G.; SPIES, T.A., and HARDING, D., 1999. Lidar remote sensing of the canopy

structure and biophysical properties of Douglas-fir western Hemlock forests, *Remote Sensing of Environment,* 70, 339–361.

LOHR, U., 1997. Digital elevation models by laserscanning principle and applications, *Proceedings of the Third International Airborne Remote Sensing Conference and Exhibition,* Copenhagen, 174–180.

MEASURES, R.M., 1984. *Laser Remote Sensing—Fundamentals and Applications,* Krieger Publishing Co., Malabar, FL, 510p.

MCCLUNG, F.J. and HELLWARTH, R.W., 1962. Giant optical pulsations from ruby, *Journal of Applied Physics,* 33, 828–829.

NIMA, 2000. *Department of Defence World Geodetic System 1984 - Its Definition and Relationships with Local Geodetic Systems, NIMA Technical Report,* Third Edition.

PEREIRA, L.M.G. and WICHERSON, R.J., 1999. Suitability of laser data for deriving geographical information. A case study in the context of management of fluvial zones, *ISPRS Journal of Photogrammetry and Remote Sensing,* 54, 105–114.

PETZOLD, B.; REISS, P., and STOSSEL, W., 1999. Laser scanning—surveying and mapping agencies are using a new technique for the derivation of digital terrain models, *ISPRS Journal of Photogrammetry and Remote Sensing,* 54, 95–104.

RITCHIE, J.C., 1995. Airborne laser altimeter measurements of landscape topography, *Remote Sensing of Environment,* 53, 91–95.

SALLENGER, A.H.; KRABILL, W.B.; SWIFT, R.N.; BROCK, J.; LIST, J.; HANSEN, M.; HOLMAN, R.A.; MANIZADE, S.; SONNTAG, J.; MEREDITH, A.; MORGAN, K.; YUNGEL, J.; FREDERICK, E.B., and STOCKDON, H., 1999a. Evaluation of Airborne laser scanning for coastal change applications: 1. Beach topography and changes, Manuscript in preparation.

SALLENGER, A.H.; KRABILL, W.B.; BROCK, J.C.; SWIFT, R.N.; JANSEN, M.; MANIZADE, S.; RICHMOND, B.; HAMPTON, M., and ESLINGER, D., 1999b. Airborne laser study quantifies El Nino-induced coastal changes, *EOS, Transactions, American Geophysical Union,* v. 80(8), 89, 92–93.

SALLENGER, A.H.; HOWD, P.; BROCK, J.; KRABILL, W.B.; SWIFT, R.N.; MANIZADE, S., and DUFFY, M., 1999c. Scaling winter storm impacts on Assateague Island, MD, VA, *Proceedings of the 4th International Symposium on Coastal Engineering and Science of Coastal Sediment Processes,* 3, 1814–1825.

SHRESTHA, R.L. and CARTER, W., 1998. Instant evaluation of beach storm damage, *Earth Observation Magazine,* March 1998, 42–44.

TSAI, B.M. and GARDNER, C.S., 1982. Remote sensing of sea state using laser altimeters, *Applied Optics,* 21(21), 3932–3940.

WEHR, A. and LOHR, U., 1999. Airborne laser scanning—An introduction and overview, *ISPRS Journal of Photogrammetry and Remote Sensing,* 54, 68–82.

ZILKOSKI, D.B.; RICHARDS, J.H., and YOUNG, G.M., 1992. Special Report—Results of the general adjustment of the North American vertical datum of 1988, *Surveying and Land Information Systems,* 52(3), 133–149.

APPENDIX A

Definitions of variables and symbols for all equations:

A_l Area illuminated by laser beam (m^2)
A_{rec} Optical receiving area of the collector (m^2).
A_{sur} Total area covered by an airborne laser survey (km^2/h).
A_{tar} Target area (m^2).
C Data acquisition rate during a survey flight (GBytes/h).
c Speed of light in the medium (km/s).
D Laser aperature width (cm).
D_{rec} Laser aperature diameter (equivalent to D) (cm).
D_{tar} Diameter of the target (m).
d Overall point density within an entire survey (points/m^2).
E Laser energy (J).
F Laser pulse repetition rate (kHz).
h Aircraft altitude above the terrain (m).
$IFOV_{diff}$ Diffraction-limited instantaneous field-of-view (m).
$IFOV_{sur}$ Surface (ground) instantaneous field-of-view (m).
M Atmospheric transmission.
n Number of swaths within a given survey.
P_{av} Average laser pulse power (W).
P_{bytes} Number of bytes recorded for a single laser shot.
P_{peak} Peak laser pulse power (W).
P_{rec} Reflected pulse power received at the collector (W).
P_{refl} Power reflected from the target (W).
P_T Transmitted laser power (W).
q Percentage of overlap between adjacent swaths in an ALS survey.
R Distance between the laser transmitter and the object surface (m).
R_{min} Minimum detectable separation between reflecting targets (m).
ΔR Range resolution of the system (cm).
s Aircraft displacement between sending and receiving a laser pulse (m).
S/N System signal-to-noise ratio.
T_f Total data acquisition time during a survey (h).
T_{sur} Time during which data was acquired for a survey strip(h).
t_L Travel time for an individual laser pulse (ns).
Δt_L Time resolution of the system (ns).
t_{min} Minimum detectable time difference between two received echoes (ns).
t_p Laser pulse duration (ns).
t_{rise} Pulse rise-time (ns).
W_{scan} Width of the scanned swath below the aircraft (m).

Greek Symbols:

θ_{inst} β Inclination angle of the local planar terrain surface (deg).
ϕ_{tar} Power density within the illuminated area (W/m^2).
γ Laser beam divergence (mrad).
λ Laser wavelength (nm).
ν Laser frequency (Hz).
θ Laser scan angle (deg).
θ_{inst} Instantaneous scan angle (deg).
ρ Target reflectance.
σ_R Absolute ranging accuracy (m).
υ Flying speed over the terrain (m/s).